Conformational Properties of the Disease-Causing Z Variant of α1-Antitrypsin Revealed by Theory and Experiment

Itamar Kass, Anja S. Knaupp, Stephen P. Bottomley, and Ashley M. Buckle

Department of Biochemistry and Molecular Biology, Monash University, Clayton, Victoria, Australia

Supporting Material

Table S1: A comparison of H-bond occupancy between wild-type and E342K mutated α1-AT.

H-bond interactions	Found in wild-type crystal structure?	Fractional occupancy during the last 200 ns of a wild-type simulation	Fractional occupancy during the last 200 ns of Z simulation
E342OE1/2:V200O	No	0	-
E342OE1/2:T203OG	Yes	0	-
E342OE1/2:K290NZ	Yes	0.52	-
K342NZ:V200O	-	-	0.33
K342NZ:T203OG	-	-	0.30
K342NZ:K290NZ	-	-	0
D341O:W194N	No	0.60	0
D341O:W194NE1	Yes	0	0.65

Table S2: The average number of H-bonds between s3A and s5A.

α1-AT variant	Following the initial 50 ns of simulations	Last 50 ns of simulations
wt	11±1	11±1
$E342K_{conf1}$	8±1	8±1
$E342K_{conf2}$	8±1	8±1
E342R	10±1	8±1
E342Q	10±1	9±1
K290E/E342K	11±1	11±1

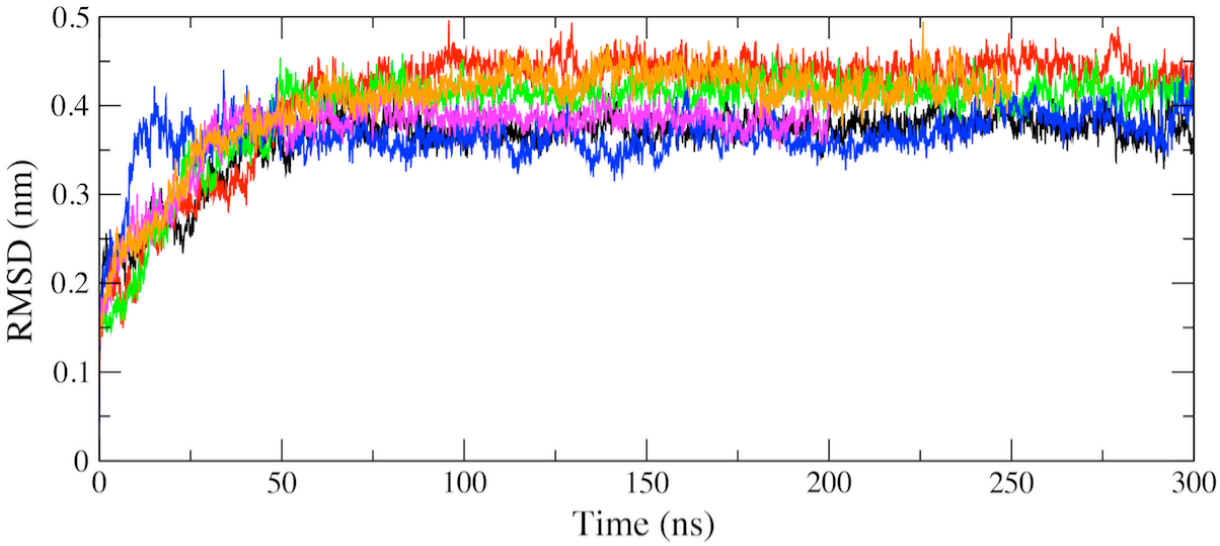

Fig. S1: Cα RMSD's as function of time for representative trajectories of wild-type (black), E342K$_{conf1}$ (red), E342K$_{conf2}$ (green), E342R (blue), E342Q (pink) and K290E/E342K (orange) mutated α1-AT. Following an initial structural rearrangement stage, during the initial 50 ns of simulations, the average Cα RMSDs were found to reach a plateau at 0.37±0.02 nm (wild-type α1-AT), 0.43±0.04 nm (E342K$_{conf1}$), 0.41±0.04 nm (E342K$_{conf2}$), 0.36±0.02 nm (E342R), 0.39±0.02 nm (E342Q) and 0.42±0.03 nm (K290E/E342K).

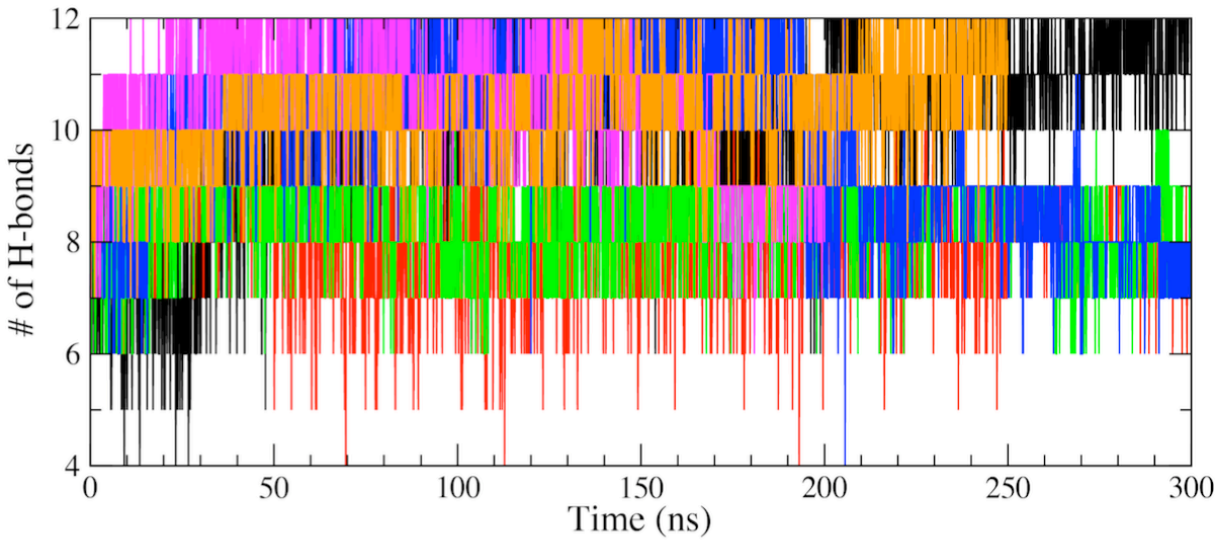

Fig. S2: Number of inter-strand H-bonds between strands s3A and s5A as a function of time for representative trajectories of wild-type (black), E342K$_{conf1}$ (red), E342K$_{conf2}$ (green), E342R (blue), E342Q (pink) and K290E/E342K (orange) mutated α1-AT. The average number of H-bonds, following the initial 50 ns of simulations, between s3A and s5A were calculated to be 11±1 (wild-type α1-AT), 8±1 (E342K$_{conf1}$), 8±1 (E342K$_{conf2}$), 10±1 (E342R), 10±1 (E342Q) and 11±1 (K290E/E342K).

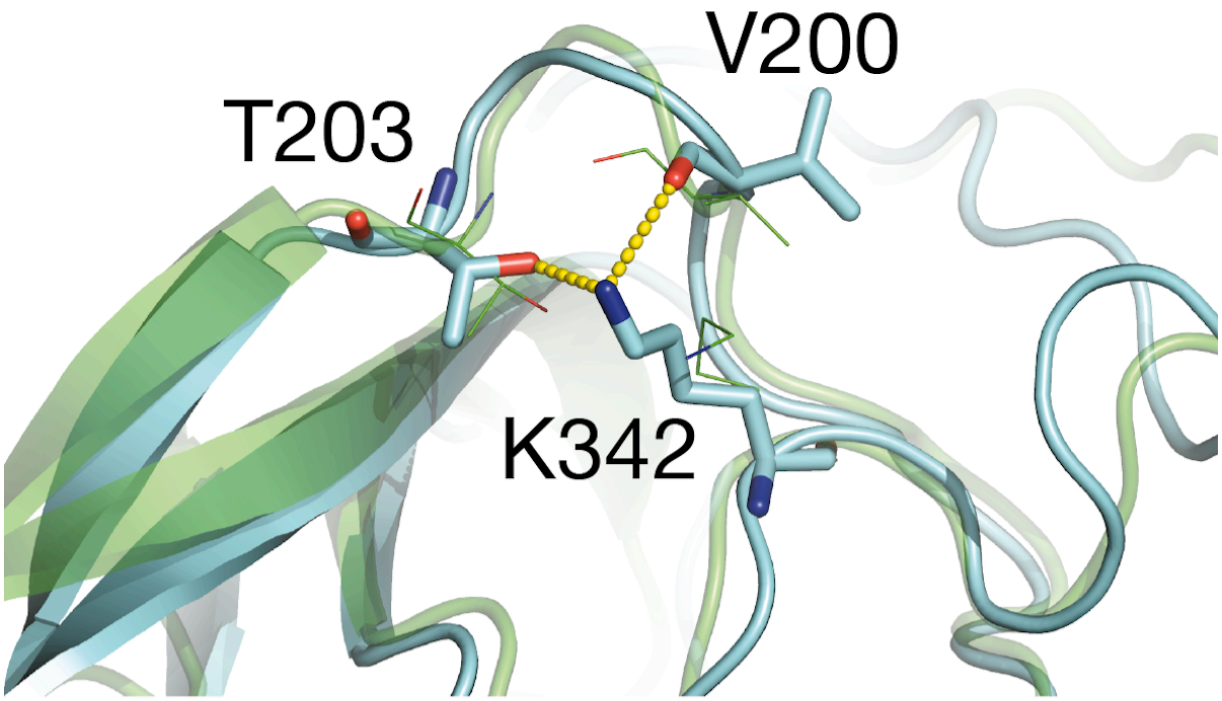

Fig. S3: The proximal-hinge region of E342K mutated α1-AT (system $E342K_{conf2}$). A comparison between the starting model of $E342K_{conf2}$ mutated α1-AT (represented as green colored cartoon with residues V200, T203 and K342 drawn as lines) and its conformation after 5 ns of simulation (represented as cyan colored cartoon with residues V200, T203 and K342 drawn as sticks). The H-bonds formed between K342, T203 and V200 during the simulations are represented as yellow broken lines. The conformation of system $E342K_{conf2}$ after simulation of 5 ns is very similar to that of the starting structure of $E342K_{conf1}$.

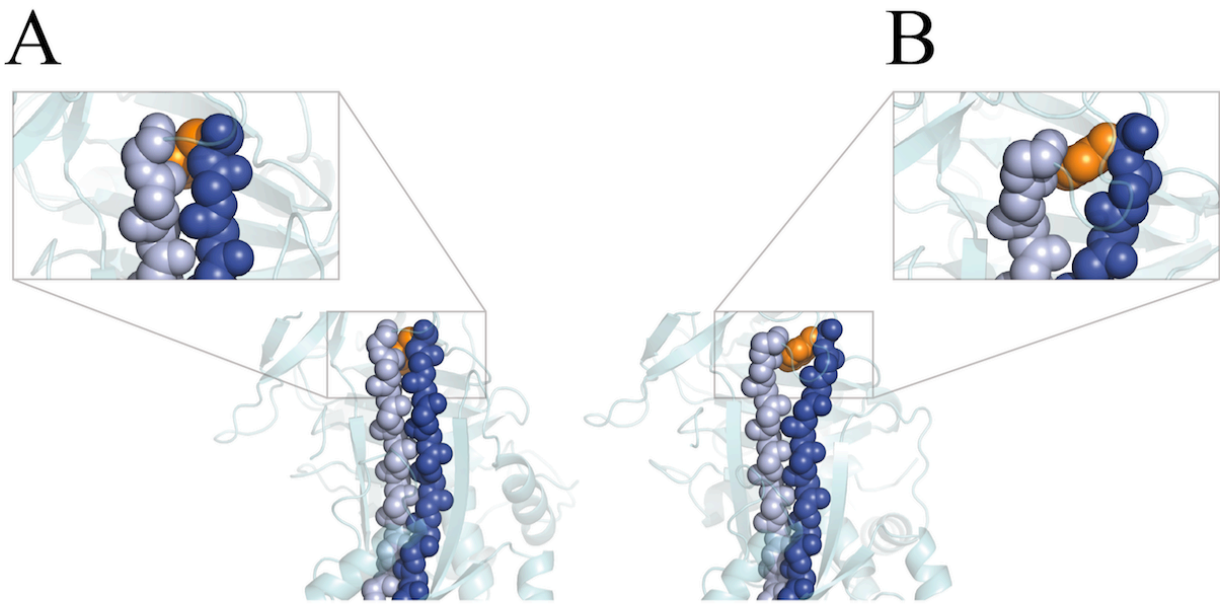

Fig. S4: A representation of time averaged structures of **(A)** wild-type and **(B)** E342K mutated α1-AT over the last 50 ns of simulation. α1-AT is represented as a cartoon, whereas backbone atoms of s3A (light blue), s5A (dark blue) and residue W194 are represented as space-filling models.

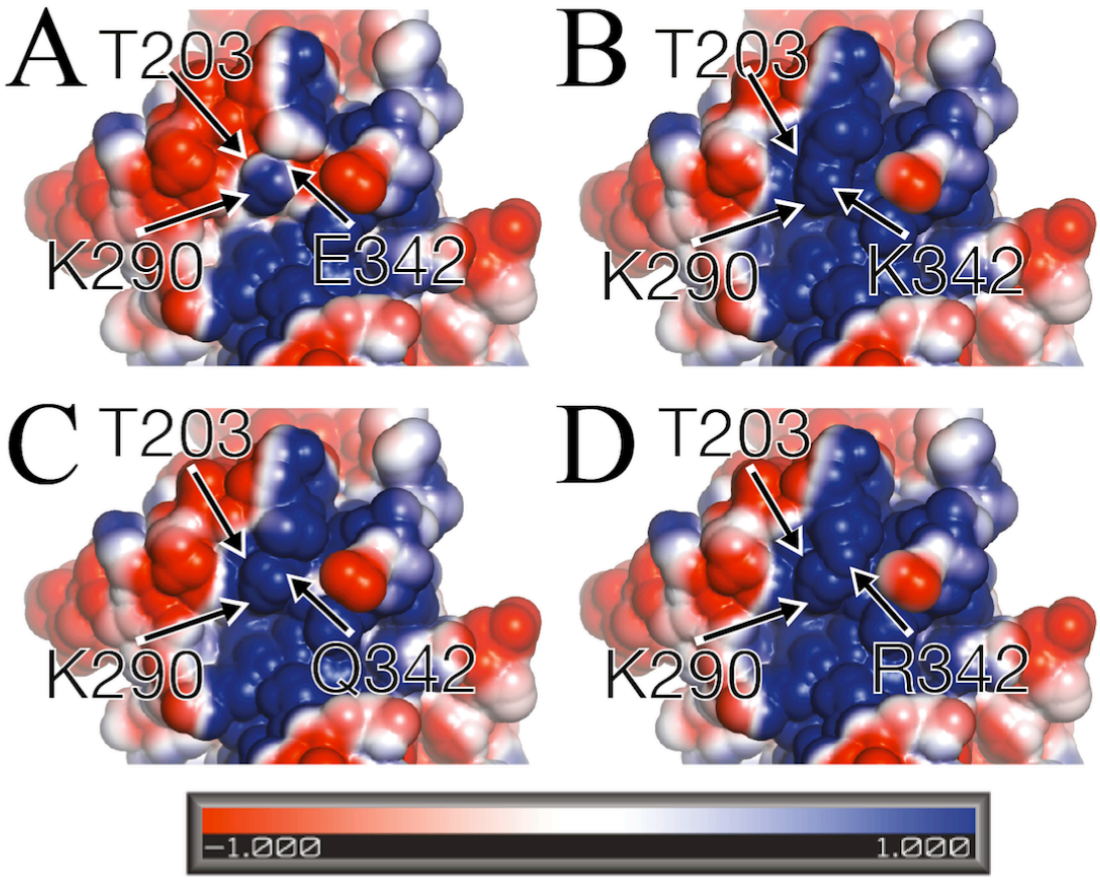

Fig. S5: Electrostatic potential of (A) wild-type, (B) E342K, (C) E342Q and (D) E342R α1-AT, mapped on solvent accessible surface of α1-AT. Color coding is according to the electrostatic potential gradient, where positively and negatively charged areas are represented in blue and red (iso-values from +1 k_bT/e_c to -1 k_bT/e_c), respectively.

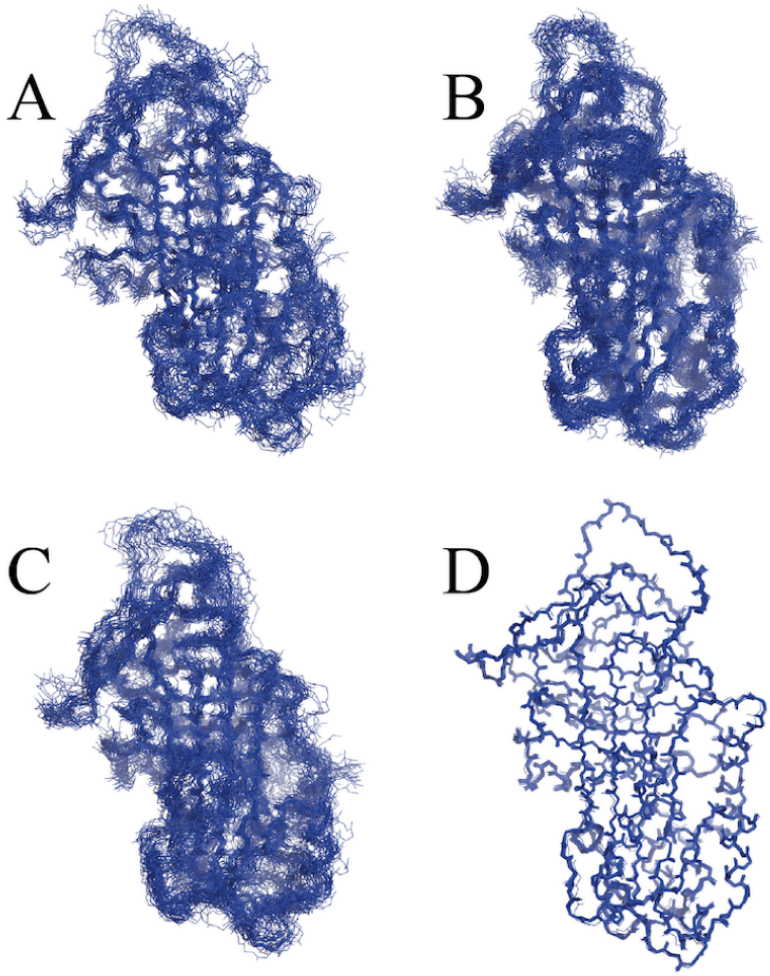

Fig. S6: Representative backbone overviews of the dynamics of different simulated systems. Superposition of 20 structures sampled every 10 ns from a 200 ns simulation of **(A)** E342Q, **(B)** 30 structures sampled every 10 ns from a 300 ns simulation of E342R, **(C)** 25 structures sampled every 10 ns from a 250 ns simulation of K290E/E342K mutated α1-AT, (**D)** 25 structures sampled every 10 ns from a 250 ns simulation of α1-AT in pseudo-crystalline environment.

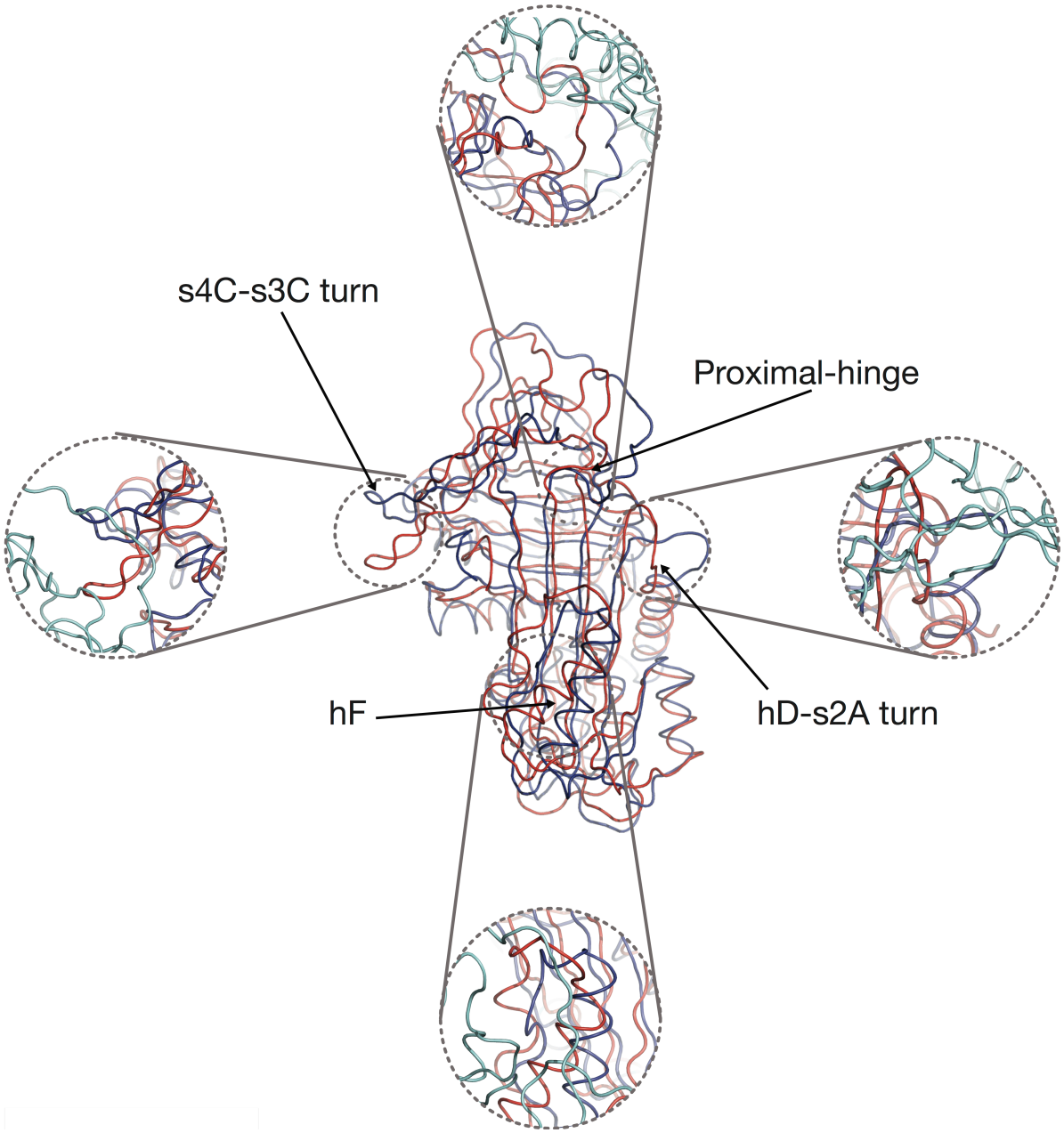

Fig. S7: A structural comparison between the crystal structure (1QLP; blue) and a time averaged structure over the last 50 ns of the simulation (red) of α1-AT. Regions with large structural differences are highlighted and enlarged in inserts, namely s3C-s4C turn, the proximal-hinge, hD-s2A turn and hF. In each insert, the crystal contacts (within 0.4 nm) are shown in cyan.

Movie S1: A movie of a 300 ns representative trajectory of wild-type α1-AT in solution. The movie contains snapshots of every 100 ps of the simulation, smoothed for visualization purposes. H-bonds are represented as broken lines.

Movie S2: A movie of a 300 ns representative trajectory of Z α1-AT in solution. The movie contains snapshots of every 100 ps of the simulation, smoothed for visualization purposes. H-bonds are represented as broken lines.

Movie S3: A movie of a 300 ns representative trajectory of E342R α1-AT in solution. The movie contains snapshots of every 100 ps of the simulation, smoothed for visualization purposes. H-bonds are represented as broken lines.

Movie S4: A movie of a 200 ns representative trajectory of E342Q α1-AT in solution. The movie contains snapshots of every 100 ps of the simulation, smoothed for visualization purposes. H-bonds are represented as broken lines.

Movie S5: A movie of a 250 ns representative trajectory of the double mutant K290E/E342K α1-AT in solution. The movie contains snapshots of every 100 ps of the simulation, smoothed for visualization purposes. H-bonds are represented as broken lines.